radiation is beamed into a wide but hollow conical radiation pattern. The emission then reflects the rotation of the source in that a remote observer first detects radiation from one side of the emission cone and then the other [for a review, see Smith, 1976; Carr et al., 1982; Goldstein and Goertz, 1982]. Dulk [1965] concluded that an emission cone angle of 79° worked well for the Io controlled sources. Goldstein et al. [1979] came to similar conclusions for the Io independent sources. Because radiation emitted from the back side of Jupiter cannot reach Earth, one would expect that the phase of Io would always be greater than 90°, but less than 270°. In fact, radiation from Io-B is often received at Io phases less than 90°. This introduces an unexplained asymmetry in the occurrence probability of the Io phase dependent source. In this paper we propose a new explanation of this asymmetry.

The asymmetry has been known for some time, and several authors have offered a variety of explanations for it. Dessler and Hill [1979], following earlier ideas [see, e. g., Goldreich and Lynden-Bell, 1969], pointed out that the difference between the sub-Io longitude and the longitude of the footpoint of the Io flux tube (IFT) is about 30° when the sub-Io longitude is 230° (using the GSFC/O_4 model for the global Jovian magnetic field [Acuña and Ness, 1976]), which is about what is needed. However this effect is in fact canceled by the rather large azimuthal deviations of the magnetic field from the meridional plane in the relevant sub-Io longitudes. Piddington and Drake [1968] considered the bending of the magnetic field by Io and estimated the propagation time of hydromagnetic waves from Io to the Jovian ionosphere. They assumed a velocity of propagation along the Io flux tube of 500 km/s, or a propagation time of about 20 minutes. According to recent models deduced from Pioneer 10 and 11 and Voyager 1 and 2 data, the Alfvén velocity along the IFT is almost equal to the velocity of light, except in the Io torus and in

A THEORY OF THE IO PHASE ASYMMETRY OF THE JOVIAN DECAMETRIC RADIATION

Kozo Hashimoto*

and

Melvyn L. Goldstein

Code 692, Laboratory for Extraterrestrial Physics

Interplanetary Physics Branch

NASA/Goddard Space Flight Center

Greenbelt, MD 20771

August 1982

*Permanent address: Department of Electrical Engineering, Kyoto University, Kyoto 606, Japan. NAS/NRC Resident Research Associate, NASA/GSFC.

ABSTRACT

We propose an explanation of an asymmetry in the occurrence probability of the Io-dependent Jovian decametric radiation. Io generates stronger Alfvén waves toward the south when it is in the northern part of the torus. This wave then generates decametric radiation in the northern ionosphere after it reflects in the southern ionosphere. The asymmetry then results from computing the propagation time of the Alfvén wave along this trajectory. The ray paths of the decameter radiation are calculated using a three-dimensional ray tracing program in the Jovian ionosphere. Variations in the expected probability plots are computed for two models of the Jovian ionosphere and global magnetic field, as well as for several choices of the ratio of the radiated frequency to the X-mode cutoff frequency.

1. Introduction

The Jovian decametric radiation, or DAM, extends in frequency from below a few megahertz to nearly 40 MHz. It is well known that the probability that a remote observer will receive radiation from Jupiter at decameter wavelengths is a critical function of the central meridian longitude (CML) of the planet as seen by the observer. In 1964 Bigg discovered that the phase of the moon, Io, controls the occurrence probability of the most intense decameter storms (Io phase is defined as the angular departure of Io from superior conjunction as seen by an observer). A second component is independent of Io phase, but is observed at central meridian longitudes close to those of the Io phase dependent component. The occurrence probability of DAM is often shown in two dimensional plots in which the axes are central meridian longitude (in System III) and Io phase. The occurrence probability is then indicated by varying shades of grey or by contours of increasing probability. The most prominent features in the occurrence probability plots are the Io phase dependent sources; the main source (Io-A, phase of Io ~ 240° and CML ~ 230°) and the early source (Io-B, phase of Io ~ 90° and CML ~ 150°). In addition, there are Io phase independent features at nearly the same CML's as for the Io A and B sources as well as an additional Io-dependent source at phase of Io ~ 240° and CML ~ 300° (source C). Other minor features exist which are described in some detail in the recent extensive review of decameter phenomenology by Carr et al. [1982].

One of the most appealing explanations for the observation that the decameter radiation comes primarily from two regions in CML and from two positions in Io's orbital phase is the idea first proposed by Dulk [1965] that decameter

radiation is beamed into a wide but hollow conical radiation pattern. The emission then reflects the rotation of the source in that a remote observer first detects radiation from one side of the emission cone and then the other [for a review, see Smith, 1976; Carr et al., 1982; Goldstein and Goertz, 1982]. Dulk [1965] concluded that an emission cone angle of 79° worked well for the Io controlled sources. Goldstein et al. [1979] came to similar conclusions for the Io independent sources. Because radiation emitted from the back side of Jupiter cannot reach Earth, one would expect that the phase of Io would always be greater than 90°, but less than 270°. In fact, radiation from Io-B is often received at Io phases less than 90°. This introduces an unexplained asymmetry in the occurrence probability of the Io phase dependent source. In this paper we propose a new explanation of this asymmetry.

The asymmetry has been known for some time, and several authors have offered a variety of explanations for it. Dessler and Hill [1979], following earlier ideas [see, e. g., Goldreich and Lynden-Bell, 1969], pointed out that the difference between the sub-Io longitude and the longitude of the footpoint of the Io flux tube (IFT) is about 30° when the sub-Io longitude is 230° (using the GSFC/O_4 model for the global Jovian magnetic field [Acuña and Ness, 1976]), which is about what is needed. However this effect is in fact canceled by the rather large azimuthal deviations of the magnetic field from the meridional plane in the relevant sub-Io longitudes. Piddington and Drake [1968] considered the bending of the magnetic field by Io and estimated the propagation time of hydromagnetic waves from Io to the Jovian ionosphere. They assumed a velocity of propagation along the Io flux tube of 500 km/s, or a propagation time of about 20 minutes. According to recent models deduced from Pioneer 10 and 11 and Voyager 1 and 2 data, the Alfvén velocity along the IFT is almost equal to the velocity of light, except in the Io torus and in

the Jovian ionosphere. Furthermore, when Io is in the northern-most part of the torus, the effect of the bending of the magnetic field lines is almost negligible. McCulloch [1971] performed ray tracing of whistler mode waves from Io to the ionosphere and calculated both propagation times and the relative intensities to arrival points in the "coupling region" using Melrose's [1967] magnetospheric density model. McCulloch did not consider any generation mechanisms for the whistler mode waves. Furthermore, the density model that he used is not supported by recent observations. Goertz and Deift [1973] assumed that an Alfvén wave reflected in the ionosphere reaches Io in a short time and doubles the magnetic tilt. They suggested that the asymmetry could arise from reconnection at an X-type neutral point in a plasma wake of Io. Smith [1973] assumed that the plasma instability that produces DAM could be convective so that in the source region very small values of the group velocity could lead to long delays (more than 10 minutes would be required) in the escape of the radiation into the magnetosphere.

The most detailed comparison between the observed occurrence probability and the assumed beaming pattern of the Io dependent source has been carried out by Thieman and Smith [1979]. They assumed that radiation emerged in a thin conical sheet centered on the magnetic field line at the point of its intersection with the Jovian ionosphere. Any reflection or refraction caused by the ambient plasma was neglected, but they did include occultation by the planet. They found that if the source region was located along a field line 20° ahead of Io (the "lead angle") the asymmetry could be accounted for. The best agreement with observations was obtained using a cone angle of 80°. In this paper we propose an explanation of this lead angle in which we include the effects of wave refraction in the Jovian ionosphere and incorporate a model of Alfvén wave propagation through the Io plasma torus. The basis for

this model is given in section 2. Three dimensional ray tracing is performed in order to explain the occurrence probability map and to evaluate conditions for wave generation in the Jovian ionosphere including constraints on the wave normal angles and on the ratio of the generated frequency to the right hand cutoff frequency. The ray tracing calculation is explained in section 3 and the results of the calculation are compared with observations in section 4. In section 5, we present our conclusions.

2. Io phase asymmetry

Neubauer [1980] has shown that because of the existence of the Io plasma torus, the unipolar current between Io and the Jovian ionosphere described by Goldreich and Lynden-Bell [1969] is in fact carried by large amplitude Alfvén waves (or Alfvén current wings). It has been suggested by many authors [Gurnett and Goertz, 1981; Goldstein et al., 1982; among others] that the strong parallel electric fields in these "kinetic" Alfvén waves [Hasegawa and Chen, 1976; Hasegawa and Mima, 1978] are the origin of the keV electrons that are thought to generate DAM.

One of the striking observations made by the Planetary Radio Astronomy (PRA) experiment on Voyagers 1 and 2 was the discovery that most of the decameter radiation has a dynamic spectrum which resembles nested parentheses, or arcs, on a frequency-time plot [Warwick et al., 1979]. The arc pattern was shown to be consistent with Dulk's [1965] emission cone model by Pearce [1981], Staelin [1981], and Goldstein and Thieman [1981]. Gurnett and Goertz [1981] proposed that the discreteness of the arc pattern could be a result of multiple reflections of the standing Alfvén wave system [but also see Lecacheux et al., 1981]. The propagation time of the Alfvén waves has

recently been calculated by Bagenal [1982], and we make detailed use of her calculations in the discussion below. The intensity of the Alfvén waves generated by a satellite was calculated in a linear treatment by Drell et al. [1965]. Neubauer's [1980] work is its extension to the nonlinear (large amplitude) regime [for reviews, see Goldstein and Goertz, 1982; Hill et al., 1982]. It was found that both the magnetic field intensity and the power in the generated Alfvén waves are approximately inversely proportional to the Alfvén velocity, $V_A = B_o/\sqrt{(4\pi\rho)}$ where ρ is the ion mass density and B_o is the magnetic field [see Neubauer, 1980 for details], i. e., proportional to the square root of the mass density.

These calculations assumed that the density profile surrounding the satellite was constant. The wavelength of the waves perpendicular to the ambient magnetic field $\lambda_\perp$ is almost equal to the diameter of Io ($2R_{Io}$, where R_{Io} is the radius of Io). The parallel wavelength then becomes

$$\lambda_\parallel = \lambda_\perp / M_A \qquad (1)$$

where M_A is the Alfvén Mach number. Results from the Voyager 1 Plasma Science Experiment indicate that $M_A \sim 0.25$ near the peak density of the torus [Bagenal, 1982]. Therefore,

$$\lambda_\parallel \sim 8\, R_{Io} \sim R_J/5 \qquad (2)$$

where R_J is the radius of Jupiter. In less dense regions, M_A is smaller and $\lambda_\parallel$ is larger. Because the radius of the torus is almost equal to that of Jupiter, the density profile surrounding Io cannot be assumed constant. The torus density surrounding Io is significantly smaller than its peak value when

Io reaches its most distant excursions north and south of the Jovian magnetic equator [see, Warwick et al., 1979]. The Alfvén wave intensity is controlled by the mean density over at least several wavelengths. When Io is not in the center of the torus, the mean densities over several wavelengths differ considerably in the northern and southern parts of Io's excursion in the plasma torus because the wavelengths tend to be larger in the lower density regions. Because of this, the Alfvén wave intensities should differ to the north and south of Io. When Io is in the northern-most part of the torus, where strong DAM is usually received, Io sees a denser plasma in the south and a dilute plasma in the north. In this situation a stronger wave is generated southward. Because the northward directed wave is weak, it is unlikely to stimulate decameter radiation when it reaches the northern ionosphere. However, the intense southward directed wave will, after reflection in the southern ionosphere, be able to generate DAM in the northern ionosphere. Gurnett and Goertz [1981] estimated that absorption of these Alfvén waves was sufficiently weak that tens of reflections were possible before significant attenuation occurred. Let us leave aside the question of whether observable radiation will be generated in the southern hemisphere and assume that all the observed radiation originates in the northern ionosphere. This assumption is consistent with the PRA observations that most of the decameter radiation appears to originate in the northern hemisphere [see Carr et al., 1982]. In that case it is possible to evaluate the expected asymmetry if radiation occurs only after a reflection in the southern ionosphere.

The propagation time of an Alfvén wave using the WKB approximation has been calculated by Bagenal [1982] (see Fig. 7 of that paper). Her results, which may require some modification due to large density gradients in the torus, can be approximated as follows;

$$T_s \text{ (Io to southern ionosphere)} = 6.5 + 3.5 \sin \Phi \text{ (min.)}$$

$$T_n \text{ (Io to northern ionosphere)} = 7.0 - 4.3 \sin \Phi \text{ (min.)} \qquad (3)$$

where $\Phi = \Phi_{Io}$(sub-Io longitude) $- 112°$. The propagation time for the wave to reach the northern ionosphere after reflection in the southern ionosphere T is

$$T = 2T_s + T_n = 20 + 2.7 \sin \Phi \text{ (min.)} \qquad (4)$$

Io moves $0.14°$/min and Jupiter rotates $0.6°$/min, so that the apparent phase of Io changes $0.46T°$ during the propagation time. The delay angle during T minutes then becomes

$$\Delta\Phi_d = 9.6° + 1.24° \sin \Phi \qquad (5)$$

During its two traverses of the torus the wave is significantly refracted by an angle

$$\Delta\Phi_A = 40° M_A \, (1.5 + 0.5 \sin \Phi) \qquad (6)$$

where M_A is effectively 0.125 according to Fig. 8 of Bagenal [1982]. Then

$$\Delta\Phi_A = 7.5° + 2.5° \sin \Phi \qquad (7)$$

The total lead angle is an addition of (5) and (7), or

$$\Delta\Phi = 17.1^\circ + 3.74^\circ \sin \Phi \qquad (8)$$

This value is close to the 20° found by Thieman and Smith [1979] needed to give the best agreement with the observed occurrence probabilities. We now turn to consider the role of refraction of the decametric X-mode radiation in the ionosphere.

3. Three-dimensional Ray Tracing

It is commonly, though not universally, assumed that DAM is generated just above the R mode cutoff frequency f_R (i. e., the cutoff frequency of the right circularly polarized fast extraordinary mode, see, e. g., Stix [1962]) at large wave normal angles and then propagates to Earth in the extraordinary (X) mode [see the recent review by Goldstein and Goertz, 1982]. The frequencies must be higher than f_R in order that DAM can escape from Jupiter in the R-X mode. When the frequency of these waves is close to f_R, they will be refracted toward the direction of the magnetic field and thus the effective cone angle of the emission pattern becomes narrower. Waves propagating toward the planet are reflected around the ionosphere. In order to evaluate such plasma effects, three-dimensional ray tracing was performed for waves generated at various locations around the ionosphere. The numerical program is based on one prepared for ray tracing in the ionophere of Earth by Jones and Stephenson [1975], and modified for use with Jovian parameters.

In using this program it is necessary to specify a global model of the Jovian magnetic field. Most of our calculations were done using the GSFC/O_4 model [Acuña and Ness, 1976; Acuña et al., 1982], but where differences are significant, the 16 coefficient JPL octopole model with three internal terms

and one external term (I3E1) was used for comparison [Smith et al., 1976]. Both of these models are based on Pioneer 11 data. In the magnetosphere, the electron density distribution was estimated using Sentman and Goertz's [1978] electron density model. Any effects of ions were neglected. The ray tracing calculation included the oblateness of Jupiter. The radial distance to the cloud tops R (in km) was taken to be

$$R = 71372/\sqrt{(1 - 0.14371 \cos^2\theta)} \qquad (9)$$

where θ is colatitude. We have slightly modified Sentman and Goertz's density model in that we use R as defined in (9) in place of their R_J. When the radiation is propagating in the topside ionosphere, as it does near the generation region, then a model for the ionospheric electron distribution must be used. Atreya and Donahue [1976] have derived such a model based on Pioneer 10 observations. We have used a nonlinear least squares fit to the results of their model in order to obtain an analytical approximation of their results. The approximation we use is

$$N_I = 1.15 \times 10^5 \exp\left(-\frac{h - 1417}{386.3}\right) / \left[1 + \left(\frac{991}{h - 276}\right)^{4.31}\right] \qquad (10)$$

where $N_I(cm^{-3})$ is the ionospheric electron density, h is the altitude in km above the cloud tops and $N_I = 0$ for $h < 276$ km. By combining the contributions to the ionosphere model with that of the magnetosphere model we obtained a single electron density model to use in the refraction calculations. This combination is included in the fitting. The model is shown as the solid curve in Figure 1. The effects of the plasma torus are not included because the density is too low to affect the ray paths of DAM, because the maximun plasma frequency in the torus is only 0.5 MHz [Warwick et al., 1979].

The waves are launched under the following starting conditions:

1. The frequency f is set to some fraction above the local R mode cutoff frequency f_R along the Io flux tube. This fraction is varied from 0.1% to 10%.

2. Initial wave normal angles of 70°, 80°, and 90° are used.

3. The conical radiation pattern is simulated by initializing the azimuthal angle in 10° steps about the magnetic field.

Ray paths are calculated up to an altitude of 2.5 Jovian radii above the cloud tops where it is then assumed that plasma effects are negligible. The final ray direction is defined by two angles: The angle of the ray with respect to the zenographic equatorial plane (d) and the equivalent longitudinal direction A, the angle between the projection onto the equatorial plane of the ray direction and the direction of CML = 0°. Rays with $|d| < 2°$ are assumed to reach Earth. DAM is received when the line of sight to the observer is along A.

4. Comparison between ray tracing results and observations

The following calculations were performed under the assumption that DAM occurs only in the northern hemisphere and then only when Io is in the northern part of the torus.

Figure 2 is an example of a calculation for f = 22 MHz and 1.01 f_R (1% above f_R). Results are shown only for sub-Io longitudes between 120° and 270° where Io is in the northern part of the torus; 30° steps in sub-Io longitude were used and ray directions are computed only for a northern hemisphere source. The dashed line indicates 120° sub-Io longitude. The symbols X, Y, and Z correspond to rays initially launched with wave normal angles of 70°,

80°, and 90°, respectively. The symbols are indicated only if $|d| < 4°$ while the ray tracing was performed with 36 initial azimuthal angles. When $|d|$ is between 2° and 4° the sizes of the symbols are changed continuously (larger symbols correspond to smaller values of $|d|$). When $|d| < 2°$ the line widths of the symbols are systematically varied in four discrete steps so that thicker symbols are used for smaller values of $|d|$. The phase of Io (γ_{Io}) is calculated by the equation:

$$\gamma_{Io} = 180° + CML - \phi_{Io} - \Delta\phi \qquad (11)$$

where ϕ_{Io} is sub-Io longitude and $\Delta\phi$ is the lead angle as defined by (8). Notice that there is no contribution from sub-Io longitude 270° because there the initial condition that $f = 1.01\, f_R$ cannot be satisfied; the required ionospheric density is too low at the altitude corresponding to a 22 MHz gyrofrequency. In fact from (10), because the required altitude is $h < 276$ km, the density given by the model is zero. The solid curves in the figure show contour plots of occurrence probability at 22 MHz based on Thieman [1979]. The contours are slightly different from Thieman and Smith's [1979] because of a different smoothing method. In this figure $\Delta\phi = 0°$, that is, no lead angle is assumed. This model, of course, includes the difference between sub-Io longitude and the longitude of the IFT foot point as well as the declination of the magnetic field using the O_4 field. Note that, as expected, Io phases less than 90° are not allowed, and the results do not fit the observations.

Figure 3 includes the lead angle calculated from (8). Other parameters are the same as those of Figure 2. Io phases less than 90° are now apparent. Fairly good agreement with observations is seen especially for wave normal angles 80° and 90°. Radiation is also allowed from CML ~ 300°, Io-C. Note

that the lower part of the Io-A contour here and in Figure 2 includes radiation from the Io-independent source region and is not applicable to this model.

In Figure 4 we show the result of assuming that $f = 1.001\ f_R$ (0.1% above f_R) at 22 MHz. Now the radiation frequency is so close to f_R that increased refraction causes the effective cone angle to become smaller. Any generation mechanism which predicts that the radiation frequency is this close to f_R cannot account for the occurrence probability of DAM so long as one retains the basic hypothesis that the A and B source regions represent emission from two sides of the same conical radiation pattern. At higher ratios of f/f_R, for example $f = 1.1\ f_R$, (10% above f_R), even better agreement with observations (cf. Figure 3) is found, especially when fairly small wave normal angles (~ 70°) are used (Figure 5). However, the results corresponding to sub-Io longitude near 270° do not fit well. The source region in this longitude range is at a very low altitude, just above the peak in the ionospheric density. Furthermore, the southern edge of the radiation cone is directed toward the observer, and thus the angle $|d|$ is very sensitive to the detailed behavior of both the magnetic field and electron density models. This choice of f/f_R gives an especially good fit in the Io-C source region. This then provides a possible explanation for the predominantly right circular polarization observed from this source in the PRA data [e.g., Carr et al., 1982].

The role of refraction is emphasized in Figure 6, where, for comparison with the earlier results (Figure 3), we have artificially set the radiating frequency to 99 MHz, far above f_R. Refraction by the plasma is neglected and ray paths are frequency-independent in this case. The remainder of the parameters are identical to the case considered in Figure 3. In this case, rays can be reflected at the cloud tops, but such rays do not reach the observer.

In this way the occultation included in Thieman and Smith's [1979] calculations can be reproduced. This figure is almost identical to their Figure 5. In this case, the observations are better fit for smaller wave normal angles.

We have tried to investigate the sensitivity of our results to our particular choice of ionospheric density model by repeating some of the calculations using a model developed from Voyager 1 data by Strobel and Atreya [1982]. To include the generally higher densities found in this model, we have increased by a factor of three the magnetospheric density derived by Sentman and Goertz [1978]. This model is also shown in the dashed curve of Figure 1. The results are shown in Figure 7 for $f = 1.01\ f_R$. The higher density causes more refraction which reduces the effective cone angle. In the case of $f = 1.1\ f_R$, the result is almost same as was shown in Figure 5.

For the remainder of this discussion we return to using the Pioneer 10 density model and examine results for other frequencies. In Figure 8 we show a calculation using $f = 1.01\ f_R$ at 15 MHz. Very good agreement with the observations is seen. In this frequency range, much of the radiation from CML's greater than 220° is dominated by Io phase independent emission and cannot be treated here.

In Figure 9, we repeat the calculation at 30 MHz. The agreement with the observed occurrence probability is not so good. However, in a case of $f = 1.1\ f_R$ (Figure 10), fairly good agreement in Io-B source is obtained for wave normal angles of 70° and 80°. Discrepancy in Io-A source may be due to generation mechanism. At such high frequencies (and low altitudes) the results are very dependent on high order multipole contributions to the magnetic field. Differences between the various global field models become noticeable. In Figure 11 we have repeated the calculation at 30 MHz using the JPL octopole model for $f = 1.01\ f_R$. The agreement with the occurrence probability data is

better in some respects in this case than that for $f = 1.1\ f_R$. At still higher frequencies (~ 38 MHz) none of the magnetic field models appear capable of correctly locating the Io-B source. This has been a problem with all models of the field and has been discussed in the review by Goldstein and Goertz [1982].

5. Conclusions

We have proposed a new model to explain the observed Io phase asymmetry of the Io controlled A, B, and C decameter sources. In this model we have assumed that when Io is in the northern part of the torus an intense Alfvén wave is generated which propagates southward, reflects from the southern ionosphere, recrosses the torus and then generates DAM when it encounters the northern ionosphere. The other Alfvén wave, initially propagating northward, encounters a lower average electron density in the torus which reduces its intensity so that it will be unlikely to generate DAM when it reaches the northern ionosphere. Standing Alfvén waves were observed by the Voyager 1 magnetic field experiment in the southern hemisphere when Io was in the southern part of the torus (CML ~ 330°) [Acuña et al., 1981]. According to our theory, stronger waves can be expected in the northern hemisphere at that time. Our model suggests that the Alfvén wing which stimulates the DAM will have a higher current density than that deduced by Acuña et al. [1981]. However, when Voyager was close to Jupiter, the PRA experiment did detect DAM at nearly all central meridian longitudes [Carr et al., 1982], which indicates that the effect we are describing is probably one of degree and one which determines the intensity of DAM rather than whether any radiation is generated at all. The fact that DAM seems to be produced predominantly when Io is in

the northern half of the torus, i. e., when the tip of the northern magnetic dipole axis points toward Io, is thought to reflect the details of the emission process and goes beyond the scope of this discussion. For the same reason, in the context of this model, we cannot explain why radiation is less likely to be observed when Io is near the center of the torus, nor can this model account for the difference between the maximum radiation frequencies of the Io A and B sources. A related question for which we have no answer, is why, when Io is in the southern part of the torus and launches an intense Alfven wave northward (or southward), DAM is not likely to be observed. These problems are probably intimately related to the plasma emission mechanism rather than the wave propagation. Finally, the location of the Io-B source at high frequencies is not particularly well explained in this model.

This paper also presents the first three-dimensional ray tracing calculations of decameter radiation in the Jovian ionosphere. As a result, we are better able to provide realistic limits on some of the source conditions necessary for the generation of DAM. The best agreement between the ray tracing and the observed occurrence probability plots was found for initial wave normal angles between 80° and 90° and radiation frequencies one to ten per cent above f_R. As f/f_R increases, smaller initial wave normal angles give better fits. The upper limit on f/f_R cannot be determined from this analysis, but will have to be calculated from whatever generation mechanism proves responsible for producing DAM. Values of $f/f_R \leq 1.001$ could not adequately model the observations. The density and magnetic field models used in this study imply that in the decameter source region the ratio of the plasma frequency to the cyclotron frequency ranges between 0.02 and 0.09, which is comparable to some estimates of this ratio in the terrestrial Auroral Kilometric Radiation (AKR) source [Calvert, 1981]. These results are consistent with

recent theories on generation of DAM and AKR [Wu et al., 1982; Goldstein et al., 1982; and the review by Goldstein and Goertz, 1982]. Besides the problems mentioned above, further work needs to be done in developing a detailed theory of the generation and saturation of the Alfvén wings in the presence of an inhomogeneous medium. Use of the WKB approximation will probably not be appropriate in such an analysis.

Acknowledgments. We would like to express our appreciation for the encouragement and advice of J. K. Alexander. We are grateful to M. L. Kaiser and M. D. Desch for their comments and permission to use their ray tracing program. We express our thanks to J. R. Thieman for his kind comments and permission to use his data.

References

Acuña, M. H., and N. F. Ness, The main magnetic field of Jupiter, J. Geophys. Res., 81, 2917-2922, 1976.

Acuña, M. H., F. M. Neubauer, and N. F. Ness, Standing Alfvén wave current system at Io: Voyager 1 observations, J. Geophys. Res., 86, 8513-8521, 1981.

Acuña, M. H., K. W. Behannon, and J. E. P. Connerney, Jupiter's magnetic field and magnetosphere, in Physics of the Jovian Magnetosphere, edited by A. J. Dessler, Cambridge University Press, in press, 1982.

Atreya, S. K., and T. M. Donahue, Model ionospheres of Jupiter, in Jupiter, edited by T. Gehrels, p. 304, University of Arizona Press, Tucson, 1976.

Bagenal, F., Alfvén wave propagation in the Io plasma torus, CSR-P-82-2, Center for Space Res., MIT, Mass., submitted to J. Geophys. Res., 1982.

Bigg, E. K., Influence of the satellite Io on Jupiter's decametric emission, Nature, 203, 1008-1010, 1964.

Calvert, W., The auroral plasma cavity, Geophys. Res. Lett., 8, 919-921, 1981.

Carr, T. D., M. D. Desch, and J. K. Alexander, Phenomenology of magnetospheric radio emissions, in Physics of the Jovian Magnetosphere, edited by A. J. Dessler, Cambridge University Press, in press, 1982.

Dessler, A. J., and T. W. Hill, Jovian longitudinal control of Io-related radio emissions, Astrophys. J., 227, 664-675, 1979.

Drell, S. D., H. M. Foley, and M. A. Ruderman, Drag and propulsion of large satellites in the ionosphere: An Alfvén propulsion engine in space, J. Geophys. Res., 70, 3131-3145, 1965.

Dulk, G. A., Io-related radio emission from Jupiter, Ph. D. Thesis, University of Colorado, Boulder, Colo., 1965.

Goertz, C. K., and P. A. Deift, Io's interaction with the magnetosphere, Planet. Space Sci., 21, 1399-1415, 1973.

Goldreich, P., and D. Lynden-Bell, Io, a Jovian unipolar inductor, Astrophys. J., 156, 59-78, 1969.

Goldstein, M. L., A. Eviatar, and J. R. Thieman, A beaming model of the Io-independent Jovian decameter radiation based on multipole models of the Jovian magnetic field, Astrophys. J., 229, 1186-1197, 1979.

Goldstein, M. L., and J. R. Thieman, The formation of arcs in the dynamic spectra of Jovian decameter bursts, J. Geophys. Res., 86, 8569-8578, 1981.

Goldstein, M. L., R. R. Sharma, M. Ben-Ari, A. Eviatar, and K. Papadopoulos, A theory of Jovian decameter radiation, submitted to J. Geophys. Res., 1982.

Goldstein, M. L., and C. K. Goertz, Theories of radio emissions and plasma waves, in Physics of the Jovian Magnetosphere, edited by A. J. Dessler, Cambridge University Press, in press, 1982.

Gurnett, D. A., and C. K. Goertz, Multiple Alfvén wave reflections excited by Io: Origin of the Jovian dacametric arcs, J. Geophys. Res., 86, 717-722, 1981.

Hasegawa, A., and L. Chen, Parametric decay of "kinetic Alfvén wave" and its application to plasma heating, Phys. Rev. Lett., 36, 1362-1365, 1976.

Hasegawa, A., and K. Mima, Anomalous transport produced by kinetic Alfvén wave turbulence, J. Geophys. Res., 83, 1117-1123, 1978.

Hill, T. W., A. J. Dessler, and C. K. Goertz, Jovian magnetospheric models, in Physics of the Jovian Magnetosphere, edited by A. J. Dessler, Cambridge University Press, in press, 1982.

Jones, R. M., and J. J. Stephenson, A versatile three-dimensional ray tracing computer program for radio waves in the ionosphere, OT Rep. 75-76, U. S. Dept. Commerce, Office of Telecommunications, 1975.

Lecacheux, A., N. Meyer-Vernet, and G. Daigne, Jupiter's decametric radio emission: A nice problem of optics, Astron. Astrophys., 94, L9-L12, 1981.

McCulloch, P. M., Theory of Io's effect on Jupiter's decametric emissions, Plnet. Space Sci., 19, 1297-1312, 1971.

Melrose, D. B., Rotational effects on the distribution of thermal plasma in the magnetosphere of Jupiter, Planet. Space Sci., 15, 381-393, 1967.

Neubauer, F. M., Nonlinear standing Alfvén wave current system at Io: Theory, J. Geophys. Res., 85, 1171-1178, 1980.

Piddington, J. H., and J. F. Drake, Electrodynamic effects of Jupiter's satellite Io, Nature, 217, 935-937, 1968.

Pearce, J. B., A heuristic model for Jovian decametric arcs, J. Geophys. Res., 86, 8579-8580, 1981.

Sentman, D. D., and C. K. Goertz, Whistler mode noise in Jupiter's inner magnetosphere, J. Geophys. Res., 83, 3151-3165, 1978.

Smith, E. J., L. Davis, Jr., and D. E. Jones, Jupiter's magnetic field and megnetosphere, in Jupiter, edited by T. Gehrels, p. 788, University of Arizona Press, Tucson, 1976.

Smith, R. A., On the Io-modulated Jovian decametric radiation, Ph. D. dissertation, University of Maryland, College Park, Md., 1973.

Smith, R. A., Models of Jovian decametric radiation, in Jupiter, edited by T. Gehrels, p. 1146, University of Arizona Press, Tucson, 1976.

Staelin, J. H., Character of the Jovian decametric arcs, J. Geophys. Res., 86, 8581-8584, 1981.

Stix, T. H., The Theory of Plasma Waves, McGraw-Hill, New York, 1962.

Strobel, D. F., and S. K. Atreya, Ionosphere, in Physics of the Jovian Magnetosphere, edited by A. J. Dessler, Cambridge University Press, in press, 1982.

Thieman, J. R., A catalog of Jovian decameter radio observations from 1957 - 1978, Tech. Memo. TM 80308, NASA/Goddard Space Flight Center, Greenbelt, Md., 1979.

Thieman, J. R., and A. G. Smith, Detailed geometrical modeling of Jupiter's Io-related decametric radiation, J. Geophys. Res., 84, 2666-2674, 1979.

Warwick, J. W., J. B. Pearce, A. C. Riddle, J. K. Alexander, M. D. Desch, M. L. Kaiser, J. R. Thieman, T. D. Carr, S. Gulkis, A. Boischot, C. C. Harvey, and B. M. Pederson, Voyager 1 planetary radio astronomy observations near Jupiter, Science, 204, 995-998, 1979.

Wu, C. S., H. K. Wong, D. J. Gorney, and L. C. Lee, Generation of the auroral kilometric radiation, J. Geophys. Res., 87, 4476-4488, 1982.

Figure Captions

Fig. 1. Jovian electron density models. Squares and circles indicate points adopted from the models based on Pioneer 10 [Atreya and Donahue, 1976] and Voyager 1 [Strobel and Atreya, 1982], respectively. The solid curve shows a Pioneer 10 density model used in our ray tracing based on the data shown as squares. The dashed curve shows a Voyager 1 model based on the data plotted as circles.

Fig. 2. The calculated reception pattern in CML-Io phase plane for 22 MHz and $f = 1.01\ f_R$. Initial wave normal angles are 70° (X), 80° (Y), and 90° (Z). The GSFC/O_4 magnetic field model and the Pioneer 10 electron density model are used. Contour plots shows smoothed occurrence probability for the same frequency based on Thieman [1979]. The contour interval for this and all subsequent contour plots is 0.2 starting at 0.1.

Fig. 3. Identical with Figure 2, but the lead angle defined by (8) is assumed in this and the following figures.

Fig. 4. Identical to Figure 3 except that $f = 1.001\ f_R$.

Fig. 5. Identical to Figure 3 except that $f = 1.1\ f_R$.

Fig. 6. Identical to Figure 3, but refraction is neglected. Ray paths are independent of frequency. Contours are the probablity for f = 22 MHz.

Fig. 7. Identical to Figure 3, but the Voyager 1 density model is used.

Fig. 8. Identical to Figure 3 except that f = 15 MHz.

Fig. 9. Identical to Figure 3 except that f = 30 MHz ($f = 1.01\ f_R$).

Fig. 10. Identical to Figure 9 except that $f = 1.1\ f_R$.

Fig. 11. Identical to Figure 9, but the JPL magnetic field model is used.

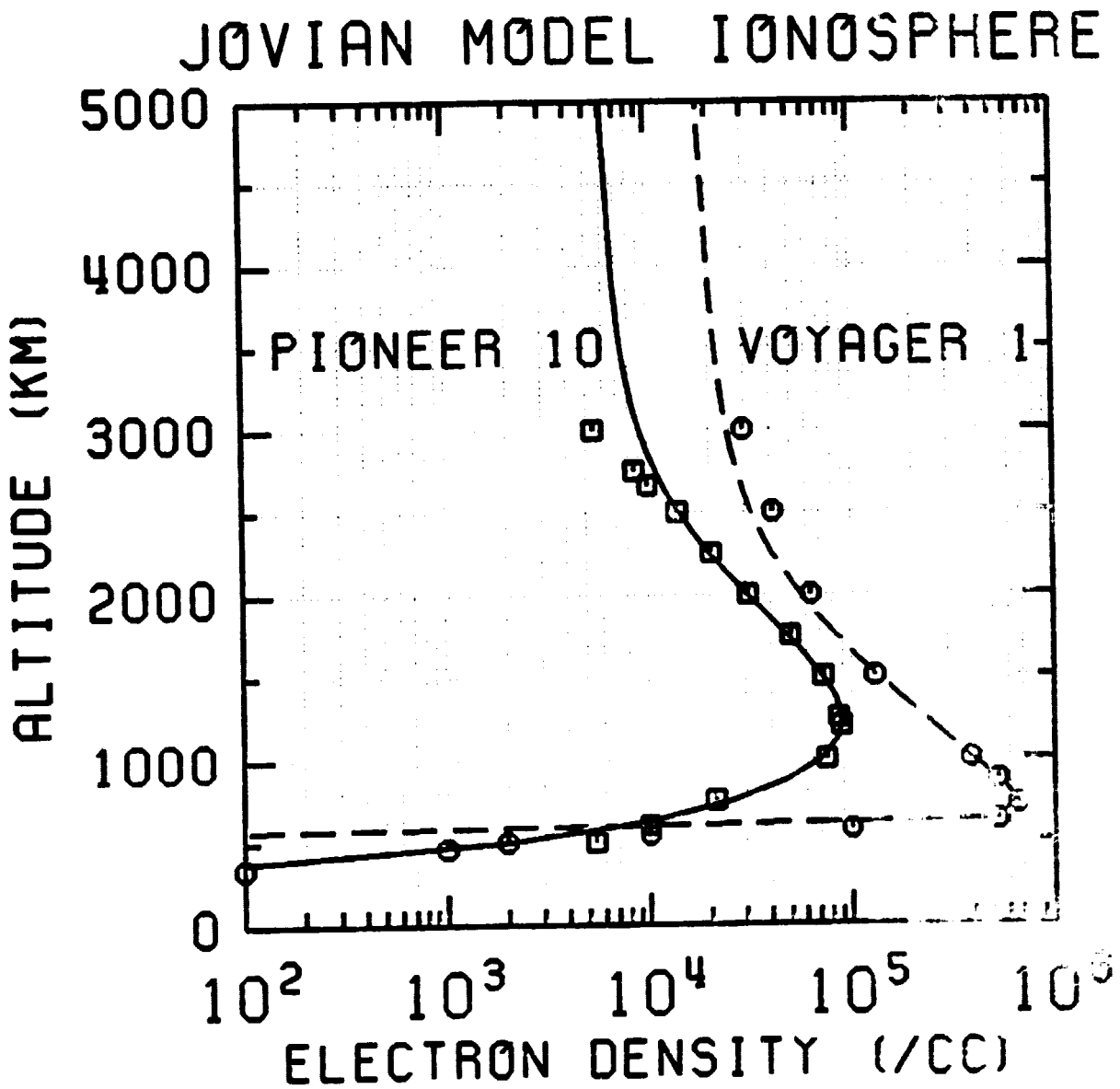

Figure 1

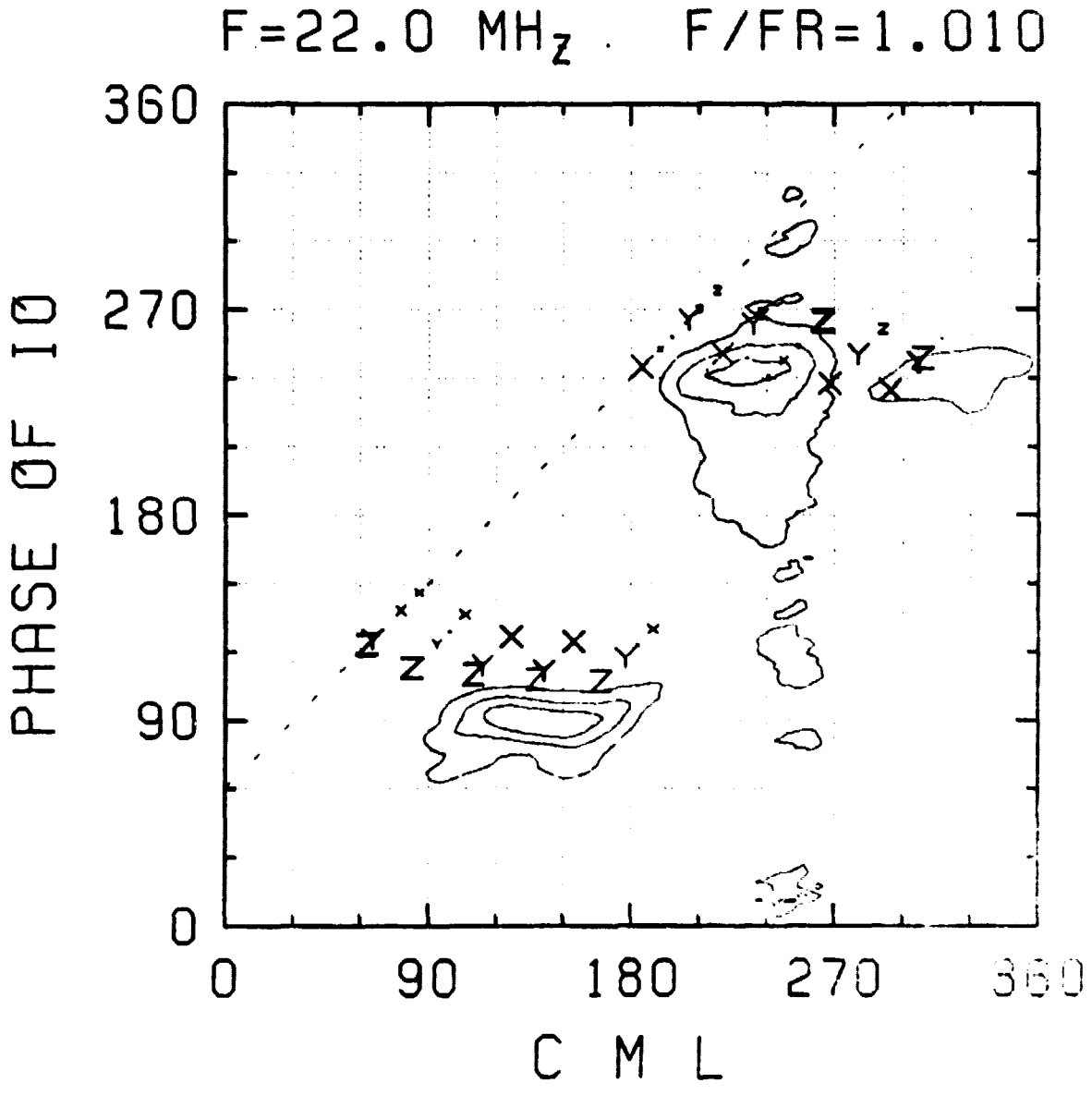

Figure 4

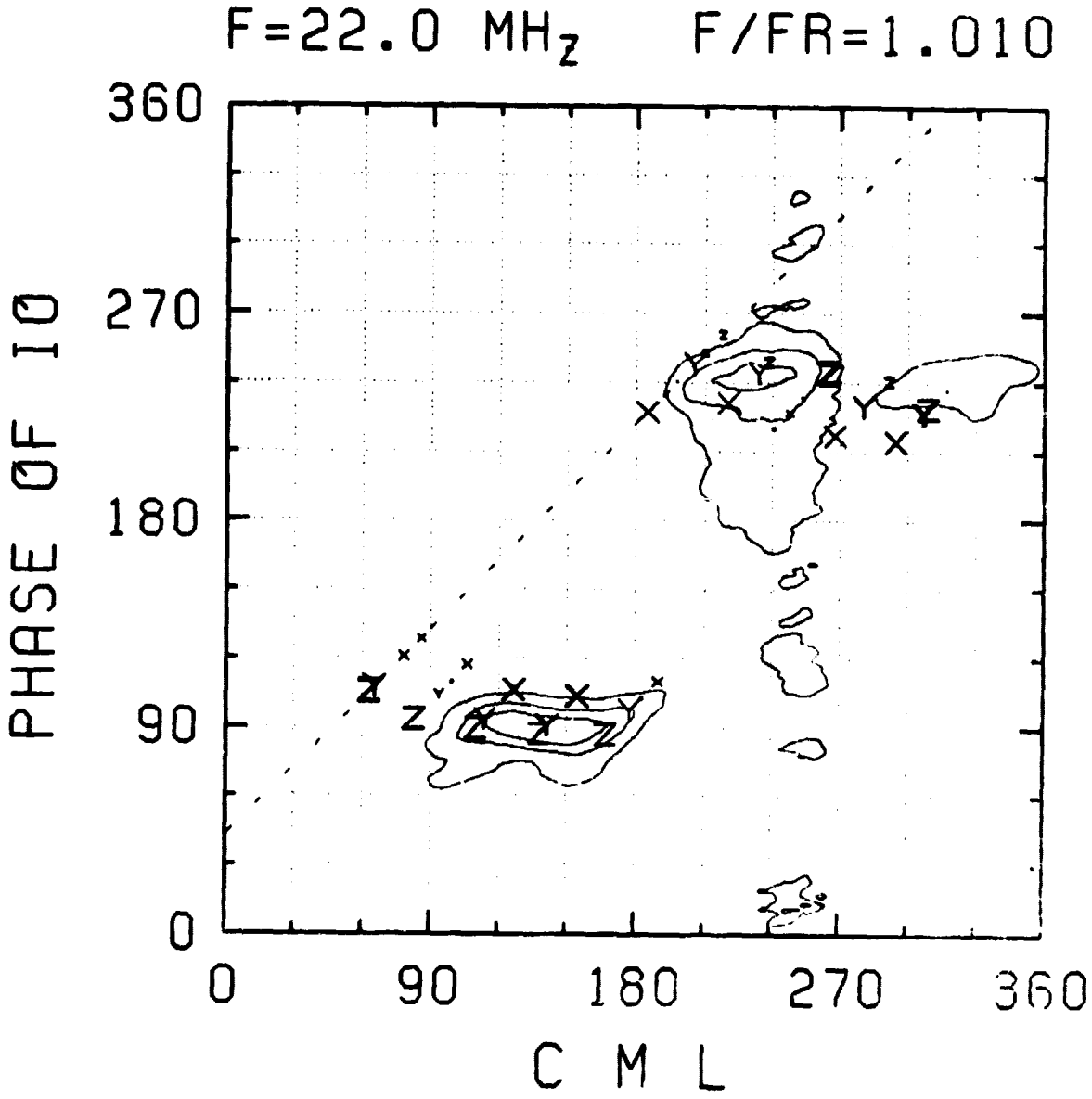

Figure 3

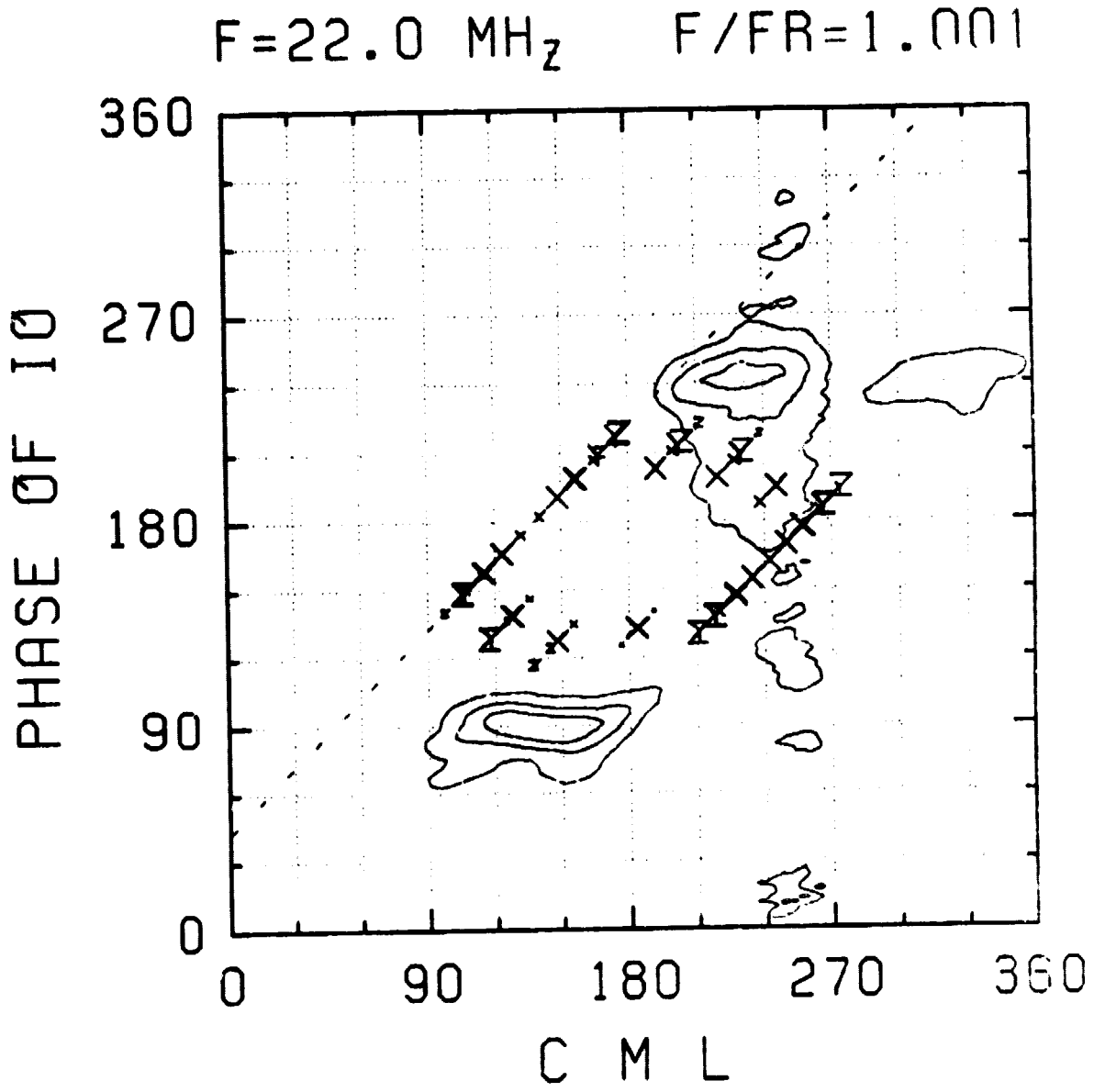

Figure 4

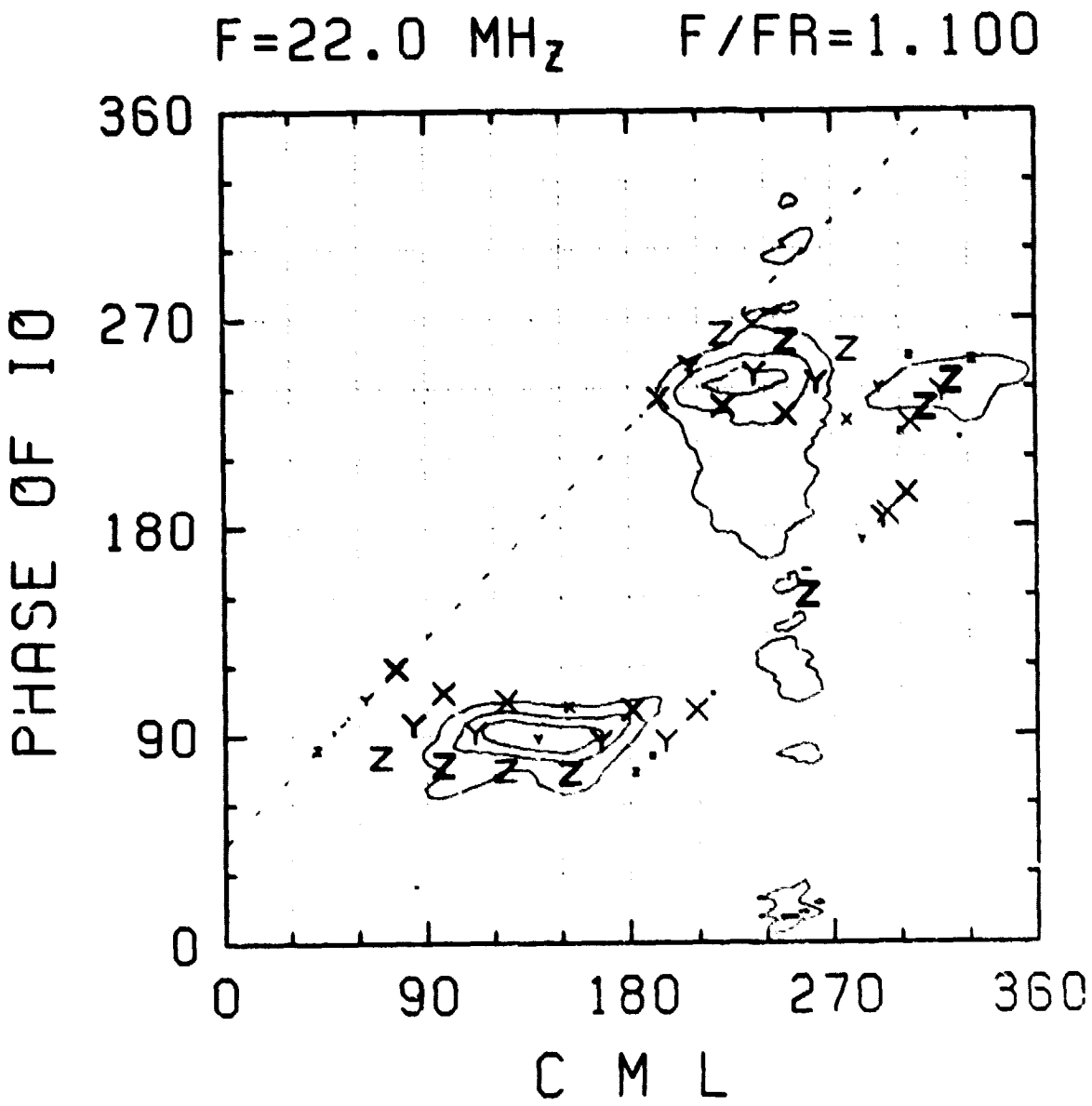

Figure 5

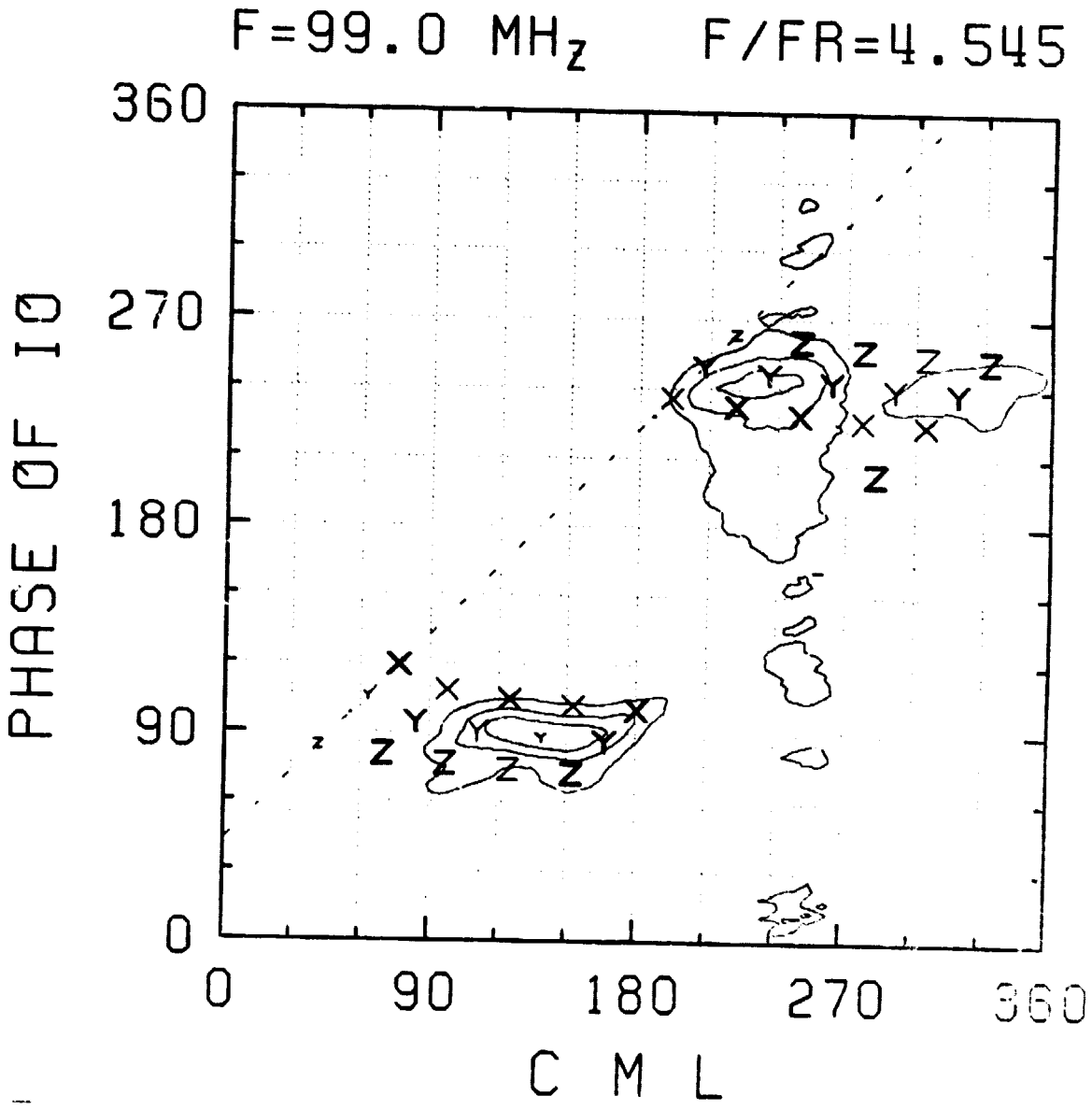

Figure 6

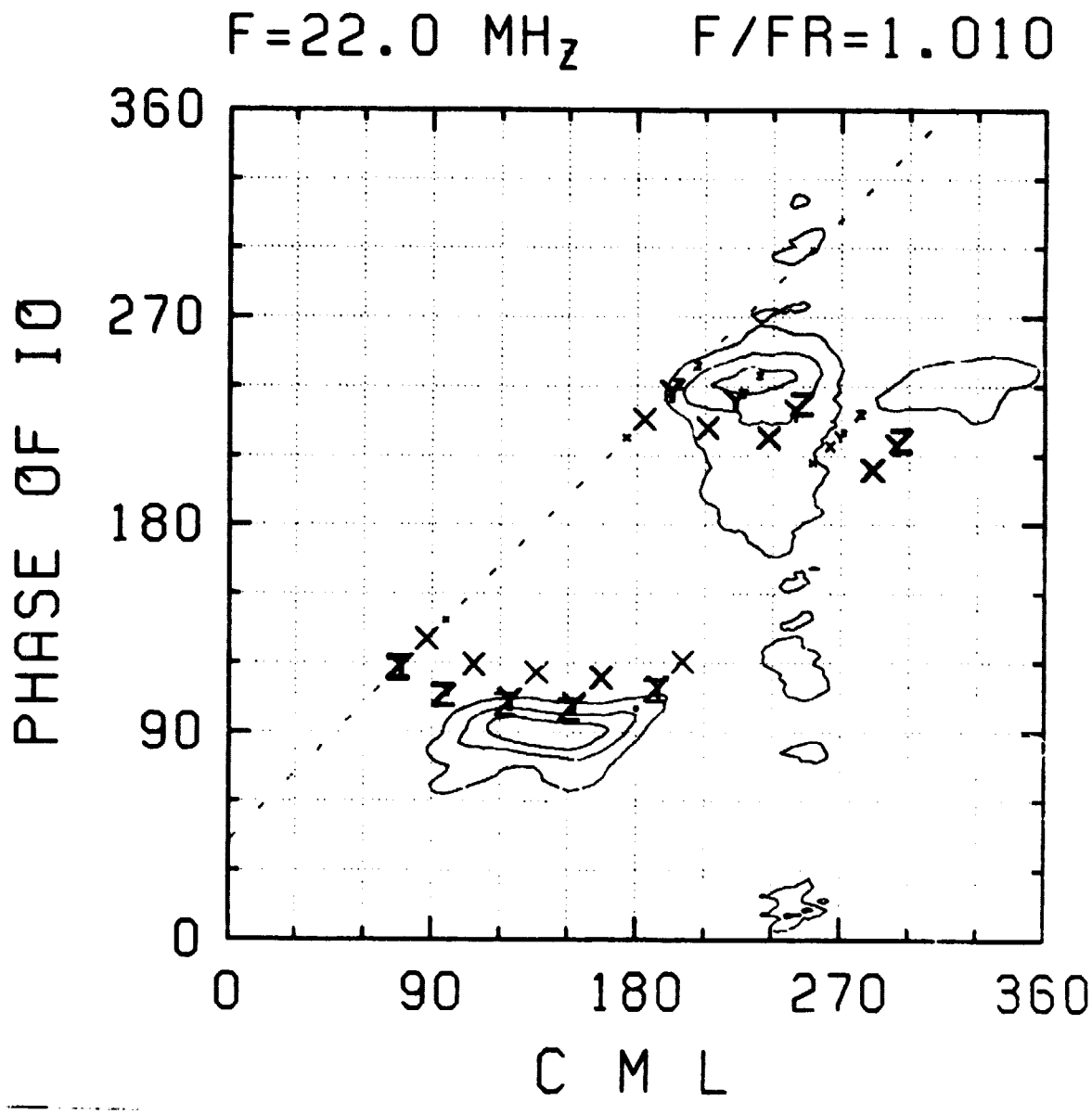

Figure 7

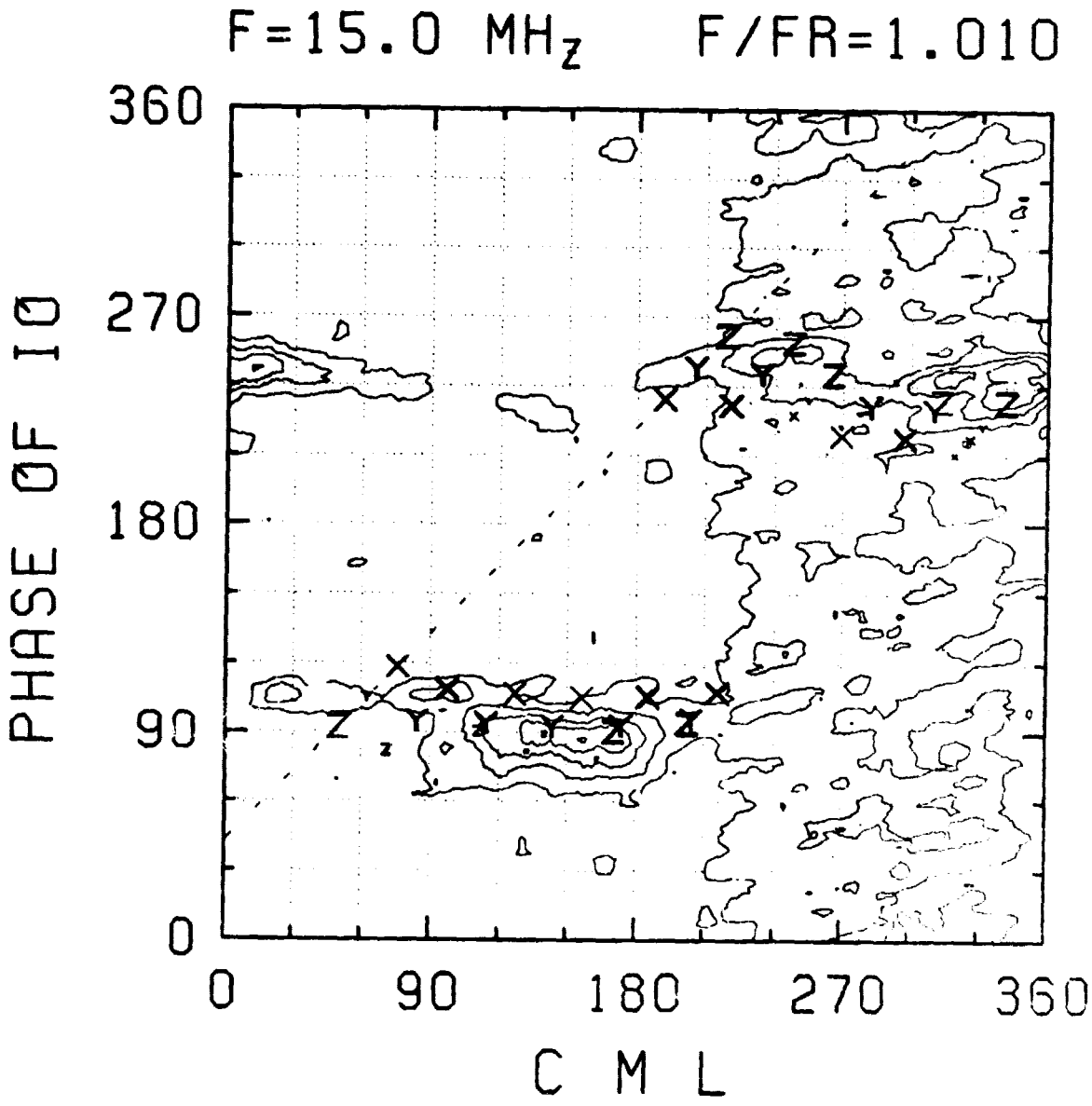

Figure 6

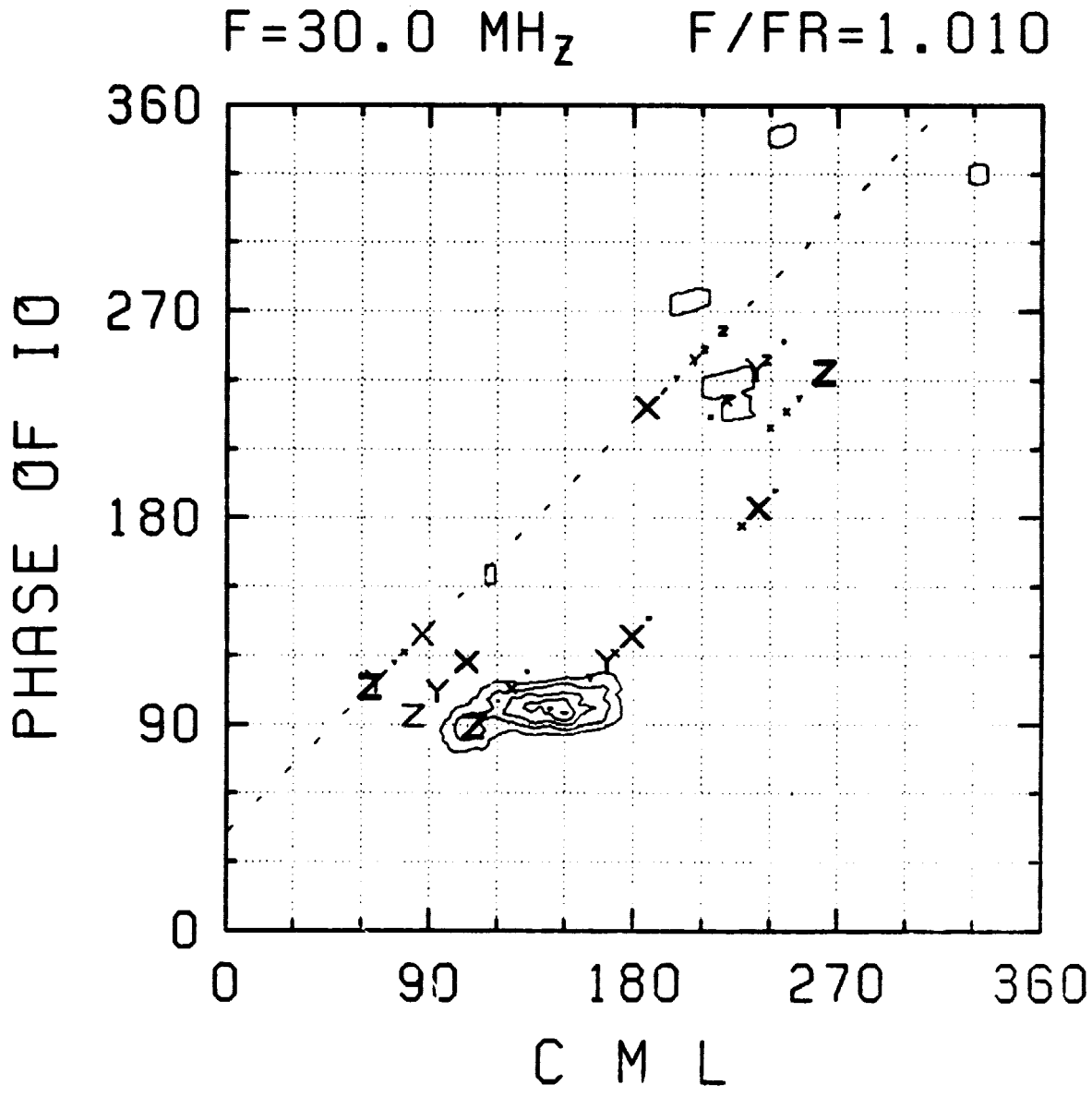

Figure 9

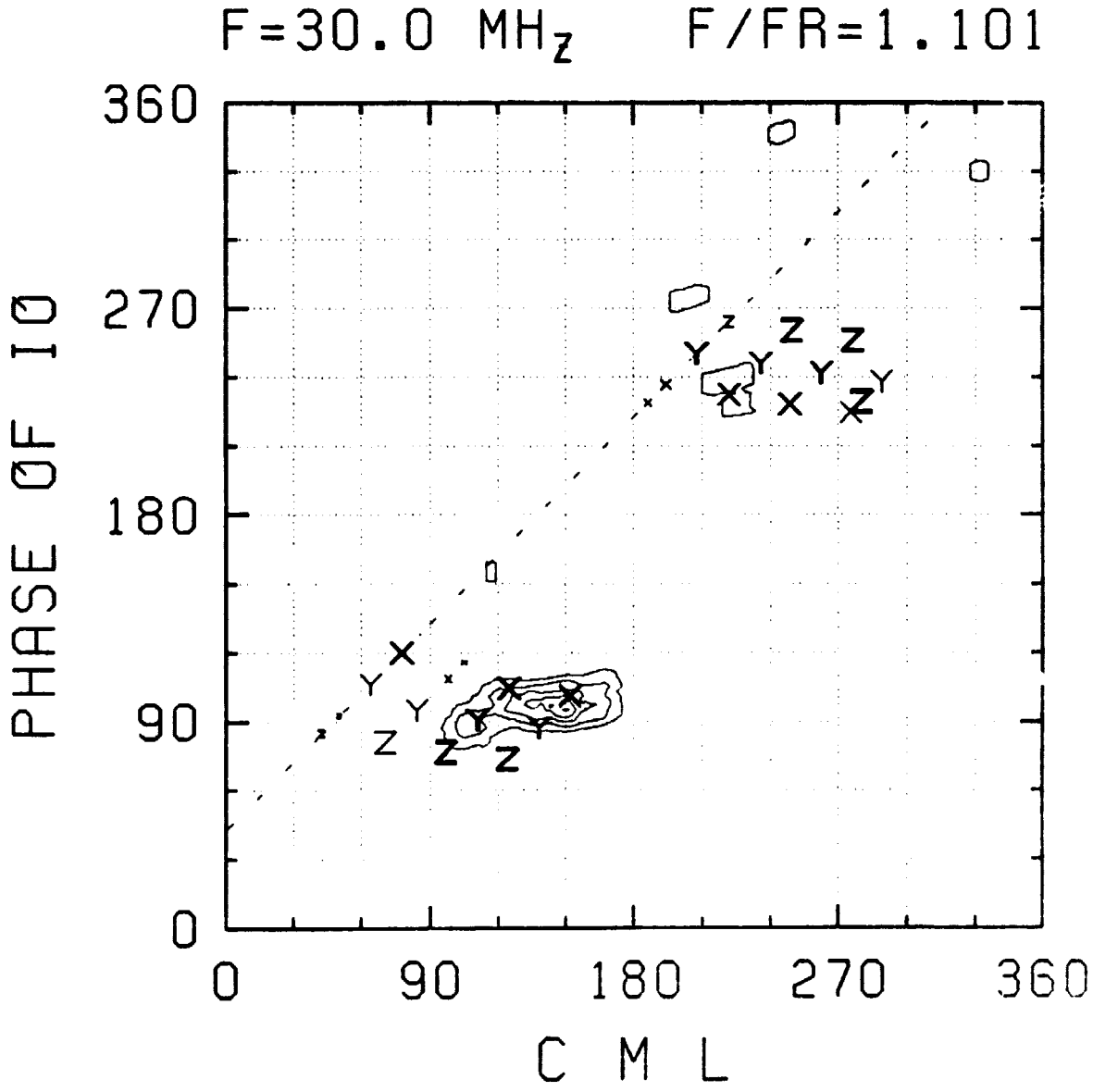

Figure 10